Revista Brasileira de Parasitologia Veterinária
Brazilian Journal of Veterinary Parasitology
ISSN 1984-2961 (Electronic)
www.rbpv.org.br

Short Communication

Feline parasitic pneumonia caused by *Troglostrongylus brevior:* a case report

Pneumonia parasitária felina causada por *Troglostrongylus brevior*: relato de caso

Orinta Vilkelienė[1]*; Dmitrij Kvitka[1]; Martinas Jankauskas[1]; Greta Rudenkovaitė[1]

[1]Lithuanian University of Health Sciences, Dr. L. Kriaučeliūnas Small Animals Clinic, Faculty of Veterinary, Veterinary Academy, Kaunas, Lithuania

How to cite: Vilkelienė O, Kvitka D, Jankauskas M, Rudenkovaitė G. Feline parasitic pneumonia caused by *Troglostrongylus brevior*: a case report. *Rev Bras Parasitol Vet* 2026; 35(4): e011126. https://doi.org/10.1590/S1984-29612026050.

Abstract

Nematodes represent an important etiological factor in verminous bronchopneumonia in domestic cats. Traditionally, *Aelurostrongylus abstrusus* and *Capillaria aerophila* were considered the principal parasitic species colonizing feline respiratory tract. However, in recent years, the clinical relevance of *Troglostrongylus brevior* has been increasingly recognized. This report describes a feline case characterized by chronic cough and persistent rhinitis lasting for four months. Thoracic radiography and ultrasonography revealed pulmonary alterations consistent with pneumonia. Routine hematological and copromicroscopic examinations yielded no significant findings. Definitive diagnosis was achieved through bronchoalveolar lavage (BAL) sampling followed by duplex polymerase chain reaction (PCR), which confirmed parasitic pneumonia attributable to *T. brevior*. Therapeutic management consisted of a topical spot-on formulation containing imidacloprid 40 mg and moxidectin 4 mg, administered on days 1 and 28. Clinical reassessment was performed on days 28, 56, 84, 112, and 140 post-treatment initiation. By day 140, all clinical signs had resolved completely. Follow-up thoracic radiographs and lung ultrasonography demonstrated no pathological changes. To the authors' knowledge, this is the first case report describing confirmed feline troglostrongylosis in Lithuania. Future studies should further investigate the epidemiological significance of cats in *T. brevior* infection, including the prevalence and distribution of the parasite within feline populations.

Keywords: *Troglostrongylus brevior*, feline lungworm, parasitic pneumonia, bronchoalveolar lavage, thoracic radiography, thoracic ultrasonography.

Resumo

Nematódeos são importantes agentes da broncopneumonia parasitária em gatos domésticos. Tradicionalmente, *Aelurostrongylus abstrusus* e *Capillaria aerophila* eram considerados os principais parasitos respiratórios felinos. Contudo, a importância clínica de *Troglostrongylus brevior* tem sido cada vez mais reconhecida. Este relato descreve um gato com tosse crônica e rinite persistente durante quatro meses. Radiografia torácica e ultrassonografia revelaram alterações compatíveis com pneumonia, enquanto exames hematológicos e copromicroscópicos de rotina não apresentaram achados relevantes. O diagnóstico foi obtido por lavagem broncoalveolar seguida de PCR duplex, confirmando pneumonia parasitária causada por *T. brevior*. O tratamento consistiu em imidacloprida 40 mg e moxidectina 4 mg tópicas nos dias 1 e 28. Reavaliações realizadas até o dia 140 demonstraram resolução completa dos sinais clínicos, sem alterações patológicas em radiografias torácicas ou ultrassonografia pulmonar. Até onde se sabe, este é o primeiro relato de troglostrongilose felina confirmada na Lituânia. Estudos futuros devem avaliar a prevalência e distribuição de *T. brevior* em populações felinas.

Palavras-chave: *Troglostrongylus brevior*, verme pulmonar felino, pneumonia parasitária, lavado broncoalveolar, radiografia torácica, ultrassonografia torácica.

Received July 14, 2026. Accepted October 5, 2026.
*Corresponding author: Orinta Vilkelienė. Tilžės Str. 18, 47181 Kaunas, Lithuania, Phone: +37067435794, e-mail: orinta.vilkeliene@lsmu.lt.
Assistant Editor: Alynne da Silva Barbosa

This is an Open Access article distributed under the terms of the Creative Commons Attribution license, which permits unrestricted use, distribution, and reproduction in any medium, provided the original work is properly cited.

Introduction

Lungworms are recognized as significant contributors to respiratory disease in domestic cats. While *Aelurostrongylus abstrusus* has long been established and extensively studied worldwide, *Troglostrongylus brevior* has only gained scientific attention in recent decades. This species appears to exhibit greater pathogenicity than *A. abstrusus*, resulting in more severe clinical manifestations and posing a potentially fatal risk, particularly in young cats (Traversa et al., 2010, 2021). Historically, *T. brevior* was considered endemic in domestic cats only within regions inhabited by the European wildcat (*Felis silvestris*), the natural host of this parasite. However, recent findings have documented its presence on four islands where the European wildcat is absent (Traversa et al., 2021).

The increasing clinical relevance and expanding geographic distribution of troglostrongylosis in domestic cats highlight the need for improved diagnostic and therapeutic strategies. Adult *T. brevior* worms reside in the bronchi and bronchioles of infected hosts. Female worms deposit eggs that hatch into first-stage larvae (L1) within the respiratory tract of definitive hosts. Like all metastrongyloid parasites, *T. brevior* has an indirect life cycle involving gastropods (slugs or snails) as intermediate hosts, where development proceeds to the infective third-stage larva (L3). Because cats rarely prey upon terrestrial mollusks, transmission to the definitive host is largely facilitated by paratenic hosts such as rodents, birds, reptiles, and amphibians. Clinical signs of *T. brevior* infection resemble those caused by other lungworms, yet this nematode demonstrates higher pathogenicity, particularly in kittens and young cats. Troglostrongylosis may lead to catarrhal bronchitis and interstitial pneumonia, conditions that can be fatal in juvenile animals, whereas older cats often exhibit subclinical infections. Adult *T. brevior* worms obstruct bronchioles and induce extensive pulmonary hemorrhage, congestion, edema, and parenchymal hepatization, thereby reducing the surface area available for gas exchange. Upper respiratory signs, including ocular-nasal discharge and sneezing, are also frequently reported in troglostrongylosis (Crisi et al., 2018; Diakou et al., 2019; Morelli et al., 2021). Importantly, *T. brevior* poses an additional threat to feline health due to its potential for vertical transmission, a route not observed in *A. abstrusus* infections (Bezerra-Santos et al., 2020; Morelli et al., 2021). The aim of the present study is to describe a clinical case of feline troglostrongylosis in which the causative nematode was identified using DNAbased diagnostic tools rather than routine fecal microscopy, and to report a novel multimodal imaging approach combining thoracic radiography and ultrasonography for monitoring parasitic pneumonia.

Case presentation

Patient Description

A 7monthold male mixedbreed cat, recently adopted from a shelter and weighing 3.2 kg, was presented to the Dr. L. Kriaučeliūnas Small Animal Clinic, Kaunas, Lithuania with a onemonth history of chronic cough, abdominal breathing, and nasal obstruction. The patient had no history of travel abroad.

Case History and Physical Examination Results

According to the anamnesis, the cat had been vaccinated against feline calicivirus, feline herpesvirus, feline panleukopenia, and rabies. Castration and routine deworming had not been performed. The patient was housed indoors and had regular contact with another cat. The diet consisted of dry food supplemented with canned food. Appetite, water intake, defecation, and urination were reported as unremarkable. At presentation, the cat exhibited sneezing accompanied by mucopurulent nasal discharge. Clinical examination revealed pink mucous membranes with a capillary refill time of 1 second. Vital parameters included a heart rate of 180 beats per minute, a respiratory rate of 36 breaths per minute, costo–abdominal breathing, and a rectal temperature of 39.8°C. Pulmonary auscultation demonstrated rough bronchovesicular breath sounds. No additional abnormalities were detected on physical examination. Based on the patient's history and clinical examination findings, the differential diagnosis list included pneumonia (parasitic, bacterial, fungal, or aspiration), rhinitis (bacterial, fungal, or associated with congenital malformation of the nasal structures), and nasal or nasopharyngeal polyps.

For further differentiation, thoracic imaging—including radiography and ultrasound—along with blood sampling and copromicroscopic examinations was initiated.

Imaging

Thoracic radiographs (Optica 20, Varex, The Netherlands) for further lungs investigation were performed without the use of sedation or general anaesthesia. In the ventrodorsal (Figure 1A) and left lateral (Figure 1B) views lungs were mildly hyperinflated. Diffuse mixed bronchointerstitial to patchy alveolar pulmonary patterns were identified, resulting in decreased delineation of the cardiac silhouette and large vessels (Figure 1B). Lobar sign consistent with severe atelectasis of the right middle lung lobe was also noted (Figure 1A-C). Several air bronchograms at the caudal lung lobes area and pulmonary nodule at the level of 6th rib on the left hemithorax associated with pneumonia were visible (Figure1A-C).

Vet BLUE (Veterinary Bedside Lung Ultrasound Examination) using a pointofcare thoracic ultrasound system (Mindray DC70; Hamburg, Germany) was performed. Caudal (Cd), Perihilar (Ph), Middle (Md), and Cranial (Cr) lung point views were recorded bilaterally. Diffuse interstitial syndrome, characterized by the presence of multiple vertical reverberation artifacts (Blines) (Figure 2B-D and G), was observed. In addition, multiple shred signs indicative of pulmonary consolidation were detected, most prominently in Figure 2H.

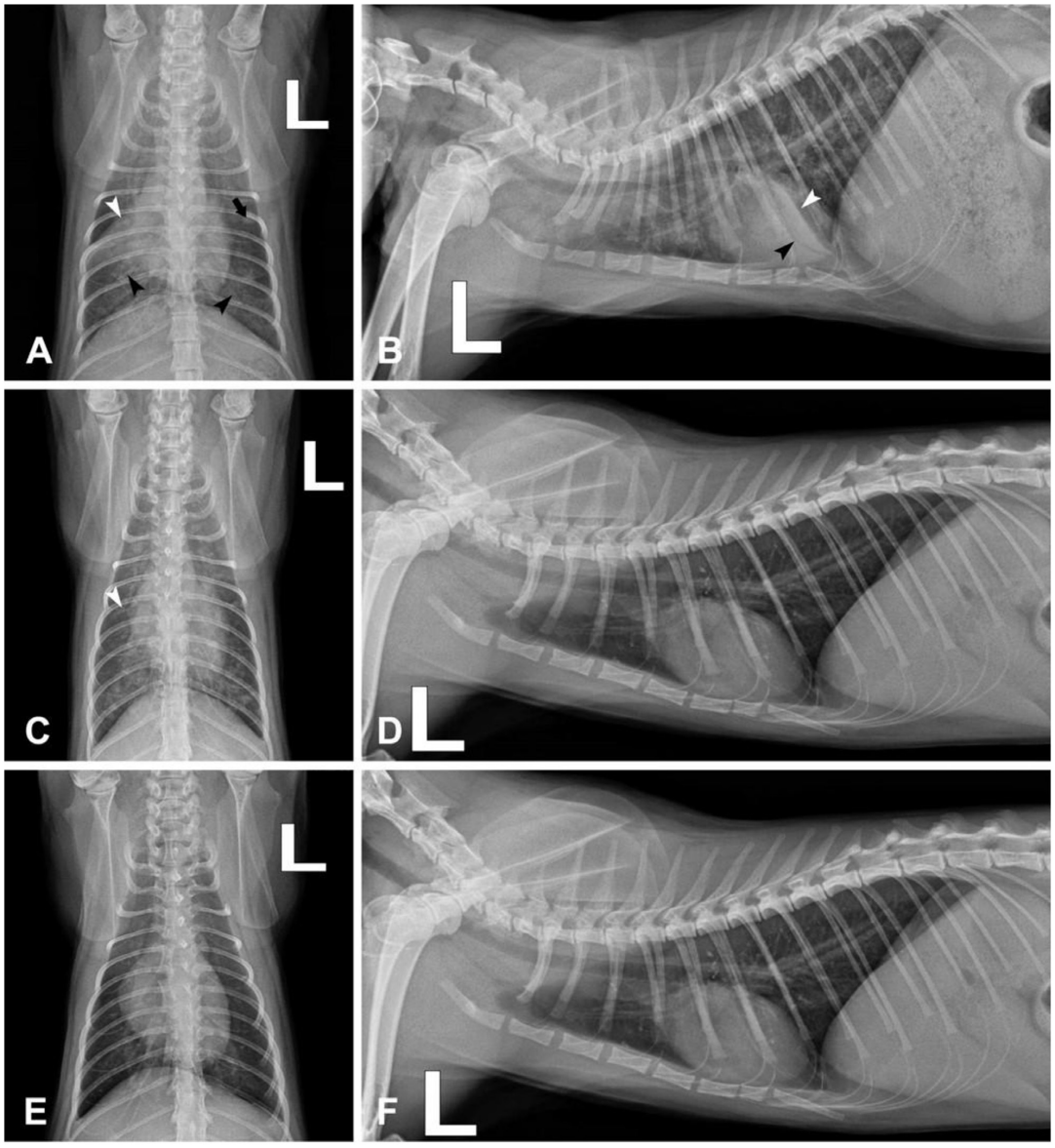


Figure 1. Ventrodorsal (A) and left lateral (B) thoracic radiographs obtained on the first day of presentation. Ventrodorsal (C) and left lateral (D) thoracic radiographs acquired on day 84 following initiation of antiparasitic therapy. Ventrodorsal (E) and left lateral (F) thoracic radiographs acquired on day 140 following initiation of antiparasitic therapy. White arrowheads indicate lobar signs, black arrowheads mark air bronchograms and black arrow indicate pulmonary nodule.

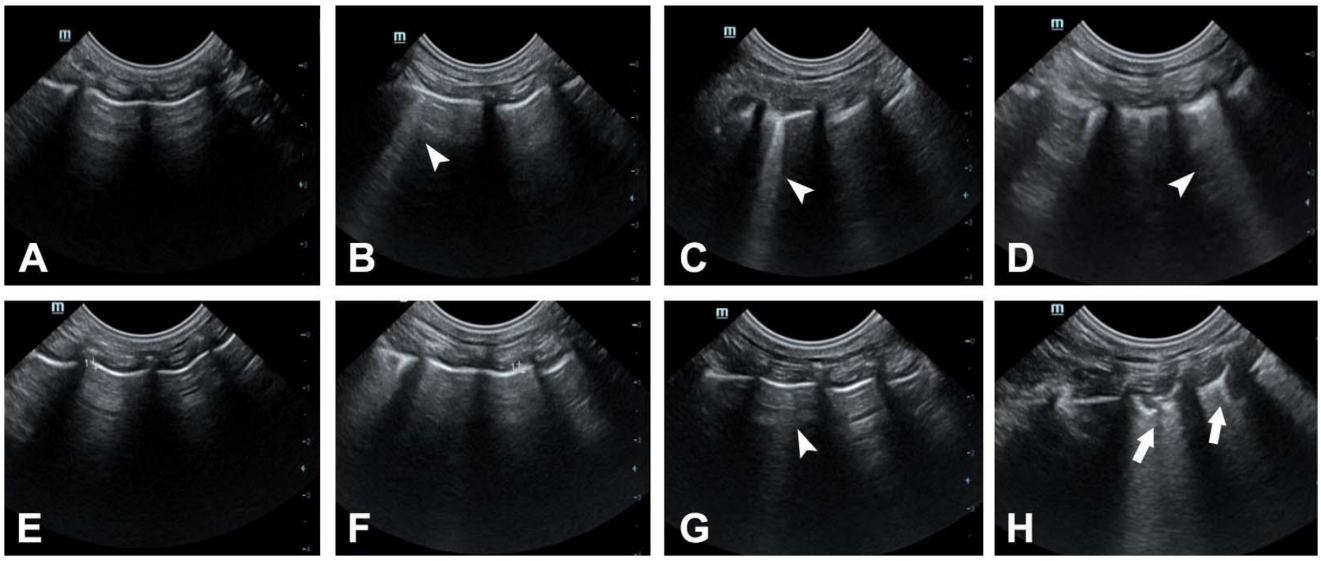


Figure 2. Left caudal (A), left perihilar (B), left middle (C), and left cranial (D) lung points, together with right caudal (E), right perihilar (F), right middle (G), and right cranial (H) lung points, recorded on the first day of presentation. White arrowheads note Blines and white arrows mark shred signs.

Laboratory Assessment

Blood samples were collected from the left cephalic vein. For complete blood count, blood was placed in an EDTA-containing tube and analyzed using the IDEXX ProCyte Dx (IDEXX Laboratories Inc., Hoofddorp, Netherlands). Blood biochemistry was performed with the IDEXX Catalyst One (IDEXX Laboratories Inc., Hoofddorp, Netherlands), and feline serum amyloid A was measured using the FUJIFILM IMMUNO AU10V (FUJIFILM Co., Tokyo, Japan) from a lithium heparin tube. White blood cells – 19.34 (reference range 2.87–17.02 ×10^9/L), monocytes – 0.96 (reference range 0.05–0.67 ×10^9/L), eosinophils – 2.08 (reference range 0.17–1.57 ×10^9/L), basophils – 0.36 (reference range 0.01–0.26 ×10^9/L), alanine transaminase (ALT) – 115 U/L (reference range 20–100 U/L), total protein – 84 g/L (reference range 54–82 g/L), and feline serum amyloid A – 10.25 µg/mL (reference range 0.00–5.49 µg/mL) were mildly increased. Red blood cell count, hematocrit, hemoglobin concentration, reticulocyte count, neutrophil count, lymphocyte count, and platelet count were within the reference ranges. Serum concentrations of albumin, alkaline phosphatase (ALP), amylase, total bilirubin, urea, calcium, phosphorus, creatinine, glucose, sodium, potassium, and globulin were also within the reference intervals. Serological testing for retroviruses (feline immunodeficiency virus and feline leukemia virus) as well as toxoplasmosis yielded negative results.

Copromicroscopic examination of fecal samples was performed using direct microscopy, flotation and Baermann technique. Three consecutive daily fecal samples, each consisting of approximately 3 g of feces, were collected and processed immediately after collection to maximize parasite recovery.

Fecal flotation was conducted by homogenizing 3 g of feces in 20 mL of saturated sodium chloride (NaCl) solution to obtain a uniform suspension. The resulting mixture was filtered through a double layer of cotton gauze (250 µm mesh) into a collection beaker. The filtered suspension was subsequently transferred into a 15 mL conical-bottom Falcon tube and centrifuged at 600 × g for 5 min. Following centrifugation, additional flotation solution was added to create a positive meniscus at the top of the tube, onto which a coverslip was carefully placed. After an incubation period of 5 min, the coverslip was removed, mounted on a glass slide, and examined microscopically at low to medium magnification (10×–20×).

The Baermann technique was performed using 3 g of feces wrapped in a double layer of gauze and suspended in a funnel containing water at room temperature. After an incubation period of 24 h, fluid from the distal portion of the funnel was collected into a Falcon tube and centrifuged at 600 × g for 5 min. Following centrifugation, the supernatant was discarded, and the sediment was microscopically examined (Colombo et al., 2022).

Flotation was used to detect nematode and protozoal ova or oocysts, while the Baermann method was employed to identify motile larvae. No parasite eggs, larvae, or oocysts were detected.

Endoscopic Evaluation and Bronchoalveolar lavage (BAL) Sampling

Due to the limited diagnostic yield of laboratory testing, an endoscopic examination was performed to further evaluate the airways. Under general anaesthesia, rhinolaryngoscopy (KARL STORZ Hopkins Rigid Scope, Germany) and tracheobronchoscopy (KARL STORZ Broncho-fiberscope, Germany) were performed. An intravenous 22G catheter was placed in the right cephalic vein. Premedication consisted of maropitant 2 mg/kg IV (Prevomax 10 mg/ml, Pfizer, Sandwich, UK) and methadone 0.3 mg/kg IV (Insistor 10 mg/ml, Richter Pharma, Wels, Austria), followed by sedation with dexmedetomidine 0.005 mg/kg IV (Dexdomitor 0.5 mg/ml, CP-Pharma, Burgdorf, Germany). Anaesthetic induction was achieved with propofol 2 mg/kg IV (Propoven 1%, Fresenius Kabi, Bad Homburg vor der Höhe, Germany), and anaesthesia was maintained with propofol 0.5 mg/kg IV. During the procedure, an infusion of 0.9% NaCl supplemented with 250 ml of 40% glucose was administered at a rate of 5 ml/kg/h IV. Following bronchoalveolar lavage (BAL) sampling, the patient was intubated with a 2.5 endotracheal tube, and 100% oxygen was delivered to maintain SpO_2 between 95–100%. Vital parameters remained within normal limits throughout anaesthesia.

During rhinoscopy, marked hyperemia of the nasopharynx, narrowed choanae, and a large amount of mucopurulent, bloody discharge were observed. Laryngoscopic findings were negligible. Tracheoscopy revealed abundant tracheal discharge consistent with mucus hypersecretion. Bronchoscopy demonstrated severe mucosal hyperemia and edema of the caudal principal bronchi. A large amount of yellowish discharge was present, with some bronchi completely obstructed (Figure 3). Access to the cranial bronchi was unsuccessful due to excessive mucus accumulation. Collapse of the right middle lobe bronchus (RM) was identified. Bronchoalveolar lavage (BAL) was performed in the region of LCD LB2D2 (left caudal lobar bronchus, second dorsal segmental bronchus) and the RM, using 4 ml/kg of sterile 0.9% sodium chloride solution. BAL samples were submitted to an accredited commercial veterinary diagnostic laboratory (LABOKLIN GmbH & Co. KG, Bad Kissingen, Germany) for cytological, mycological, bacteriological, and PCR testing for lungworms.

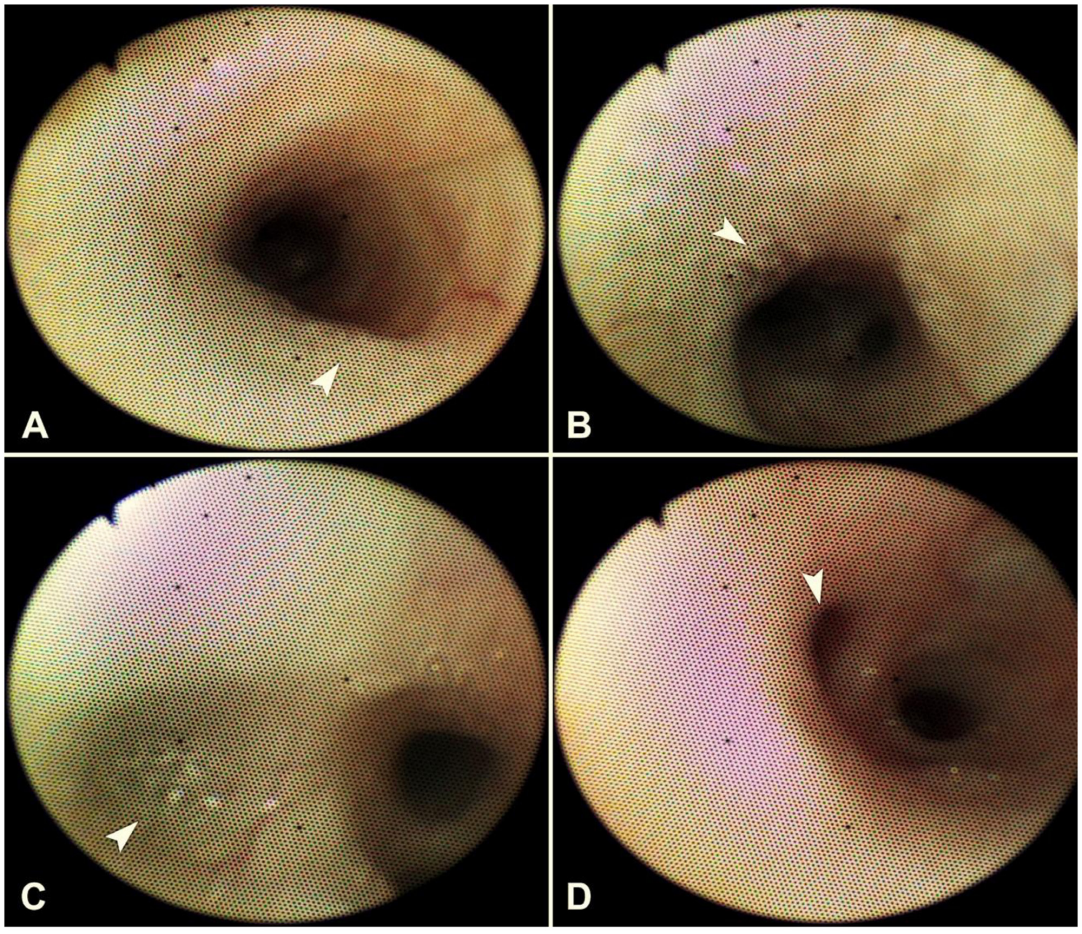


Figure 3. Tracheobronchoscopic images demonstrating severe mucus accumulation (A, B), a mucus plug (C), and bronchial collapse (D). Excessive mucus accumulation is indicated by the white arrowheads.

Detection of *T. brevior* and *A. abstrusus* DNA was performed using a laboratory-adapted duplex PCR assay. A duplex PCR assay was employed using species-specific forward primers targeting the ITS-2 region, producing amplicons of 220 bp for *A. abstrusus* and 370 bp for *T. brevior*. The assay utilized modified forward primers, *TrogloF* (5′-GCACTTGAAATCTTCGACA-3′) and *AeluroF* (5′-GCATTTATGCTAGTGATATC-3′), together with the common reverse primer *MetR* (5′-TAAGCATATCATTTAGCGG-3′). PCR was performed in 50 µL reactions containing genomic DNA, primers, dNTPs, $MgCl_2$, buffer, and DNA polymerase. Amplification conditions consisted of an initial denaturation at 95°C for 10 min, followed by 40 cycles of 95°C for 1 min, 50°C for 1 min, and 72°C for 1 min, with a final extension at 72°C for 7 min. A no-template control was included (Annoscia et al., 2014).

The PCR-positive bronchoalveolar lavage sample from the present case was not further analysed by Sanger sequencing. Assay specificity had been previously verified during laboratory validation procedures; consequently, no sequence identity analysis was performed and no GenBank accession number is available for this case.

Supportive therapy

After the procedure, the cat was hospitalized in the intensive care unit (ICU) for three days. Due to suspected bacterial pneumonia, supported by leukocytosis, thoracic imaging, and endoscopic evaluation findings, as well as suspected bacterial rhinitis, consistent with purulent nasal discharge and endoscopic findings, antimicrobial therapy was initiated with amoxicillin–clavulanate and enrofloxacin to provide broad-spectrum coverage against Gram-positive, Gram-negative, and anaerobic bacteria. Antimicrobial therapy was administered with amoxicillin–clavulanate (Synulox, Zoetis, Belgium) at 12.5 mg/kg subcutaneously (SC) every 24 hours and enrofloxacin (Enroxil, KRKA, Slovenia) at 5 mg/kg SC every 24 hours for three days. Analgesic and antiinflammatory effects were achieved with robenacoxib (Onsior, Elanco GmbH, Cuxhaven, Germany) at 2 mg/kg SC every 24 hours for three days. Highflow 100% oxygen therapy was provided continuously. For continued treatment at home, the cat was prescribed amoxicillin–clavulanate (Clavaseptin, Vetoquinol, France) at 25 mg/kg orally (PO) every 12 hours for 14 days, enrofloxacin (Enroxil, KRKA, Slovenia) at 5 mg/kg PO every 24 hours for 14 days, and inhalations of salmeterol/fluticasone (Seretide Inhaler, Glaxo Wellcome Production, France) at a 25 µg/50 µg dose every 12 hours for 7 days.

BAL results report

Cytological examination of the sample revealed low cellularity, with occasional superficial oropharyngeal epithelial cells, ciliated respiratory epithelial cells, and a mixed bacterial population. Inflammatory cells were present in low numbers and consisted predominantly of macrophages (48%), followed by eosinophils (39%), small lymphocytes (7%), and neutrophils (6%).

Testing for *Mycoplasma felis* and mycological examination yielded negative results. Bacteriological culture demonstrated a high concentration of *Stenotrophomonas maltophilia* infection. Antimicrobial susceptibility testing using the microdilution method showed susceptibility to fluoroquinolones, tetracyclines, and phenicols.

Lungworm duplex PCR testing was negative for *A. abstrusus* and positive for *T. brevior*.

Etiological therapy and outcome of the treatment

An antiparasitic treatment regimen consisting of a spoton formulation of imidacloprid 40 mg and moxidectin 4 mg (Prinocate, KRKA, Slovenia) was administered on days 1 and 28. Antimicrobial therapy consisting of amoxicillin–clavulanate and enrofloxacin was continued for a total treatment duration of 14 days, as previously described. The patient was subsequently evaluated on days 28, 56, 84, 112, and 140 following initiation of therapy. At each visit, a thorough anamnesis was obtained and a complete physical examination was performed. Thoracic radiographs and Vet BLUE examinations were repeated on days 84 and 140 to monitor pulmonary status.

Based on information provided by the owner, the patient's clinical condition improved within two weeks following initiation of antiparasitic therapy. Abdominal breathing and rhinitis resolved completely after an additional two weeks. On day 84 of treatment, thoracic radiographs demonstrated a bronchointerstitial pulmonary pattern. The lobar sign, consistent with atelectasis of the right middle lung lobe, was only mildly visible, and air bronchograms were no longer present (Figure 1C and D). Vet BLUE examination on day 84 revealed multiple distinct Blines (Supplementary Figure S1B, F and H) and several shred signs (Supplementary Figure S1D and E), findings compatible with ongoing pulmonary consolidation.

On day 140, clinical examination findings were unremarkable. Thoracic radiographs demonstrated mild pulmonary hyperinflation with only a subtle interstitial pattern. No evidence of alveolar changes or atelectasis was observed (Figure 1E and F). Vet BLUE performed on day 140 revealed normally aerated lungs, characterized by the presence of Alines (Supplementary Figure S2A, D and G). No Blines or shred signs were detected at any lung point (Supplementary Figure S2).

Despite resolution of the clinical signs and an excellent clinical condition, persistent imaging abnormalities prompted repeat bronchoscopy for further airway evaluation. On day 28 following the second dose of the antiparasitic treatment, bronchoscopy was repeated and a bronchoalveolar lavage (BAL) sample was collected. The sample was submitted to LABOKLIN for duplex PCR testing for lungworms. Results were negative, confirming complete clinical recovery from parasitic infection.

Discussion

Troglostrongylosis requires prompt diagnosis and treatment, as the disease can result in irreversible damage such as pulmonary hypertension. Furthermore, untreated animals may serve as sources of infection through the shedding of larvae (Traversa et al., 2022a). In the present case, the route of parasite transmission could not be determined. However, given the patient's history of shelter residency, vertical transmission cannot be excluded.

Field studies have demonstrated that the prevalence of *T. brevior* infection in cats varies across geographic areas; however, its occurrence is consistently reported throughout Southern Europe and the Mediterranean region. Based on the currently available literature, this appears to be the first reported case of feline troglostrongylosis in Northern Europe. Previous case reports of feline troglostrongylosis have predominantly originated from Mediterranean endemic regions (Brianti et al., 2012; Giannelli et al., 2014; Deak et al., 2017; Umur et al., 2020).

Only a few cases of *T. brevior* have been reported in Central Europe. One study found that 57.1% (4/7) of Eurasian lynxes in Germany had patent metastrongyloid infections, including infection with *T. brevior* (Haas et al., 2025). *T. brevior* larvae were identified in 1.0% (2/193) of the intermediate host slug *Arion vulgaris* collected from a public park in Austria (Penagos-Tabares et al., 2020), suggesting a potential route of transmission to stray cats. In Poland, *T. brevior* was identified in 0.5% (5/1058) domestic cats (Jańczak et al., 2026).

The occurrence of *T. brevior* in Lithuania may therefore reflect either an emerging parasite distribution or previous underdiagnosis. Diagnosis based solely on larval morphology can be challenging because first-stage larvae closely resemble those of *A. abstrusus*, potentially leading to misidentification (Annoscia et al., 2014; Crisi et al., 2018). In addition, feline lungworm infections are not routinely included in the diagnostic work-up of cats with respiratory disease, and molecular testing is rarely performed. Consequently, infections with *T. brevior* may have remained undetected in Lithuania.

Furthermore, free-roaming cats may be exposed to infected gastropod intermediate hosts and paratenic hosts, facilitating parasite transmission and creating opportunities for cross-species transmission between wild and domestic felids (Traversa et al., 2021). Future epidemiological studies investigating domestic cats, wild felids, and gastropod intermediate hosts are warranted to better evaluate the distribution, prevalence, and transmission dynamics of *T. brevior* in Lithuania and neighbouring countries.

Feces are considered the optimal biological sample for detecting L1 larvae by copromicroscopy. However, intermittent larval shedding or very low numbers of L1 larvae in feces can complicate diagnosis and lead to falsenegative results. Therefore, examination of samples from multiple defecations (e.g., three consecutive samples) may be necessary when negative results are obtained in clinically suspected cases (Salant et al., 2020; Morelli et al., 2021).

Although bronchoscopy and BAL cytology have been described in several studies, these procedures are of limited diagnostic value in cats infected with *T. brevior*. Bronchoscopic abnormalities and BAL cytological findings associated with feline lungworm infections are generally nonspecific and may overlap substantially with those observed in other feline lower airway diseases. Consequently, bronchoscopy and BAL cannot be considered reliable diagnostic methods for lungworm infection unless larvae are directly identified within the collected samples. Furthermore, both procedures are invasive and require sedation or general anaesthesia, which may pose an increased risk in clinically compromised cats. Diagnostic sensitivity may also be limited in cases with minimal pulmonary involvement, low larval burden, prepatent infection, or inadequate sample recovery (Crisi et al., 2017; Morelli et al., 2021).

The limitations of copromicroscopic and BAL cytology examination can be overcome by the use of duplex PCR assays (Crisi et al., 2018). Research suggests that pharyngeal swabs are likely the most effective samples for the molecular diagnosis of troglostrongylosis. This conclusion is supported by both experimental sensitivity data and practical considerations, including difficulties in obtaining sufficient fecal material from cats in field conditions, false negatives associated with prepatent larval migration, challenges in DNA extraction from fecal samples, and the potential presence of PCR inhibitors in stool (Morelli et al., 2021).

In the present case, a multimodal treatment protocol consisting of antiparasitic, antimicrobial, non-steroidal anti-inflammatory (NSAID), and inhaled combination therapy was implemented. The authors hypothesize that the *T. brevior*-associated parasitic pneumonia was complicated by a secondary bacterial infection, and that the comprehensive therapeutic approach contributed to the patient's successful clinical recovery. Nevertheless, the role of secondary bacterial infections in feline lungworm disease has not yet been fully elucidated, and the decision to administer antibiotics should be made on a case-by-case basis (Traversa et al., 2021).

In one study, thoracic radiographs of cats positive for *T. brevior* demonstrated predominantly interstitial and bronchial patterns. Notably, interstitial pulmonary changes were identified in an asymptomatic kitten, whereas a bronchointerstitial pattern was observed in a kitten presenting exclusively with upper respiratory tract signs, including oculonasal discharge and sneezing. These findings emphasize the importance of radiographic evaluation in cats belonging to at-risk populations (Crisi et al., 2018). Although the clinical severity of lungworm infections may only partially correspond to the extent of radiographic abnormalities, the presence of radiographic changes including vascular patterns should raise suspicion of lungworm infection in the differential diagnosis of cats, whether presenting with respiratory signs or apparently healthy but exposed to risk factors (Crisi et al., 2017).

In this study, thoracic radiographs were combined with lung ultrasonography to enhance detection of pulmonary changes localised within the surface of the lung. Ultrasonography offers several advantages over other imaging modalities for the evaluation of pulmonary parenchyma, as it is relatively inexpensive, non-invasive, minimally stressful for the patient, and comparatively straightforward to interpret with appropriate training. Computed tomography (CT) combined with airway sampling is widely regarded as the gold–standard diagnostic approach for the assessment of thoracic pathology (Morelli et al., 2021). Nevertheless, these procedures commonly require sedation or general anaesthesia, which may be contraindicated or impractical in clinically unstable patients with respiratory compromise. In such cases, point-of-care thoracic ultrasonography represents a valuable alternative diagnostic modality (Cole et al., 2021).

As awareness of troglostrongylosis increases, effective treatment options are essential for curing infected cats and interrupting the life cycle of *T. brevior*. Within the European Union, several licensed spoton formulations containing moxidectin (Diakou et al., 2019; Traversa et al., 2022b), eprinomectin (Knaus et al., 2020), or emodepside (Traversa et al., 2022a) have been demonstrated to be effective and safe against troglostrongylosis.

Conclusion

As the first molecularly confirmed case of *T. brevior* infection in a domestic cat in Lithuania, this report highlights the importance of considering *T. brevior* among the differential diagnoses in cats presenting with respiratory disease, particularly in endemic or emerging areas. Clinical and imaging findings may be nonspecific and overlap with those of other feline respiratory disorders, which can complicate diagnosis. In the present case, the absence of *T. brevior* larvae in fecal samples may have been associated with intermittent larval shedding, a low larval burden, or a prepatent stage of infection. Consequently, a comprehensive diagnostic approach, including molecular detection of *T. brevior* DNA by duplex PCR performed on bronchoalveolar lavage (BAL) samples, was crucial for confirming the diagnosis of troglostrongylosis. This enabled the timely initiation of appropriate treatment and ultimately resulted in complete clinical recovery of the patient.

In the present case, the predominant radiographic pulmonary changes associated with *T. brevior* pneumonia were a diffuse mixed bronchointerstitial and patchy alveolar pattern, with evidence of lobar consolidation and air bronchograms. Thoracic ultrasonography revealed multiple B-lines and shred signs as the most prominent abnormalities. Following the initiation of antiparasitic treatment, the patient's pulmonary status was monitored by serial thoracic radiography and ultrasonography. Progressive resolution of the pneumonia-associated abnormalities was observed, with a marked reduction in imaging findings by day 84 and complete radiographic and ultrasonographic recovery by day 140 after treatment initiation. In parallel, the clinical signs associated with pneumonia completely resolved within 14 days of treatment initiation. Further studies are warranted to better define the epidemiology and clinical significance of *T. brevior* infection in domestic cats in Lithuania.

Financial support

This research received no external funding.

Data availability

Data and information about this case are available from the corresponding author upon reasonable request.

Ethics declaration

All procedures were consented by the animal owner.

Conflict of interest

The authors declare no conflict of interest.

Author contributions

Orinta Vilkelienė: investigation and writing. Dmitrij Kvitka: supervision, revision and correction of the manuscript. Martinas Jankauskas: revision and correction of the manuscript. Greta Rudenkovaitė: investigation, writing, preparation of the manuscript. All authors contributed to the article and approved the submitted version.

References

Annoscia G, Latrofa MS, Campbell BE, Giannelli A, Ramos RAN, Dantas-Torres F, et al. Simultaneous detection of the feline lungworms *Troglostrongylus brevior* and *Aelurostrongylus abstrusus* by a newly developed duplex-PCR. *Vet Parasitol* 2014; 199(3-4): 172-178. https://doi.org/10.1016/j.vetpar.2013.10.015. PMid:24238839.

Bezerra-Santos MA, Mendoza-Roldan JA, Abramo F, Lia RP, Tarallo VD, Salant H, et al. Transmammary transmission of *Troglostrongylus brevior* feline lungworm: a lesson from our gardens. *Vet Parasitol* 2020; 285: 109215. https://doi.org/10.1016/j.vetpar.2020.109215. PMid:32862125.

Brianti E, Gaglio G, Giannetto S, Annoscia G, Latrofa MS, Dantas-Torres F, et al. *Troglostrongylus brevior* and *Troglostrongylus subcrenatus* (Strongylida: Crenosomatidae) as agents of broncho-pulmonary infestation in domestic cats. *Parasit Vectors* 2012; 5(1): 178. https://doi.org/10.1186/1756-3305-5-178. PMid:22916686.

Cole L, Pivetta M, Humm K. Diagnostic accuracy of a lung ultrasound protocol (Vet BLUE) for detection of pleural fluid, pneumothorax and lung pathology in dogs and cats. *J Small Anim Pract* 2021; 62(3): 178-186. https://doi.org/10.1111/jsap.13271. PMid:33496045.

Colombo M, Morelli S, Damiani D, Del Negro MA, Milillo P, Simonato G, et al. Comparison of Different Copromicroscopic Techniques in the Diagnosis of Intestinal and Respiratory Parasites of Naturally Infected Dogs and Cats. *Animals* 2022; 12(19): 2584. https://doi.org/10.3390/ani12192584. PMid:36230325.

Crisi PE, Aste G, Traversa D, Di Cesare A, Febo E, Vignoli M, et al. Single and mixed feline lungworm infections: clinical, radiographic and therapeutic features of 26 cases (2013-2015). *J Feline Med Surg* 2017; 19(10): 1017-1029. https://doi.org/10.1177/1098612X16670563. PMid:27694367.

Crisi PE, Di Cesare A, Boari A. Feline Troglostrongylosis: Current Epizootiology, Clinical Features, and Therapeutic Options. *Front Vet Sci* 2018; 5: 126. https://doi.org/10.3389/fvets.2018.00126. PMid:29974053.

Deak G, Ionică AM, Mihalca AD, Gherman CM. *Troglostrongylus brevior*: a new parasite for Romania. *Parasit Vectors* 2017; 10(1): 599. https://doi.org/10.1186/s13071-017-2551-4. PMid:29208009.

Diakou A, Morelli S, Dimzas D, Di Cesare A, Capelli G, Parrinello C, et al. Efficacy of a moxidectin/imidacloprid spot-on formulation (Advocate®) for the treatment of *Troglostrongylus brevior* in naturally infected cats in a field study in Greece. *Parasit Vectors* 2019; 12(1): 519. https://doi.org/10.1186/s13071-019-3760-9. PMid:31685011.

Giannelli A, Passantino G, Ramos RAN, Lo Presti G, Lia RP, Brianti E, et al. Pathological and histological findings associated with the feline lungworm *Troglostrongylus brevior. Vet Parasitol* 2014; 204(3-4): 416-419. https://doi.org/10.1016/j.vetpar.2014.05.020. PMid:24912956.

Haas M, Segeritz L, Anders O, Middelhoff TL, Myat Tun A, Hasheminasab SS, et al. Patent *Troglostrongylus brevior*-, *Aelurostrongylus abstrusus*-, *Angiostrongylus* sp.-, and *Crenosoma* sp. infections in wild Eurasian lynxes (*Lynx lynx*) and their habitat-sharing gastropod intermediate hosts. *Front Vet Sci* 2025; 12: 1515507. https://doi.org/10.3389/fvets.2025.1515507. PMid:40678497.

Jańczak D, Moroz-Fik A, Radziejewska K, Maj AK, Górecki P, Kędziorek J, et al. Prevalence of Pulmonary Nematodes in Cats and Lung Ultrasound Findings in Separate Animal Cohorts: A Coprological, Molecular and Clinical Study. *Animals* 2026; 16(4): 622. https://doi.org/10.3390/ani16040622. PMid:41751082.

Knaus M, Visser M, Mayr S, Rehbein S. Efficacy of a topical combination of eprinomectin, praziquantel, fipronil and (S)-methoprene against developing and adult *Troglostrongylus brevior* lungworms (Nematoda, Crenosomatidae) in cats. *Vet Parasitol* 2020; 277S: 100032. https://doi.org/10.1016/j.vpoa.2020.100032. PMid:34392943.

Morelli S, Diakou A, Colombo M, Di Cesare A, Barlaam A, Dimzas D, et al. Cat respiratory nematodes: current knowledge, novel data and warranted studies on clinical features, treatment and control. *Pathogens* 2021; 10(4): 454. https://doi.org/10.3390/pathogens10040454. PMid:33920104.

Penagos-Tabares F, Groß KM, Hirzmann J, Hoos C, Lange MK, Taubert A, et al. Occurrence of canine and feline lungworms in *Arion vulgaris* in a park of Vienna: first report of autochthonous *Angiostrongylus vasorum, Aelurostrongylus abstrusus* and *Troglostrongylus brevior* in Austria. *Parasitol Res* 2020; 119(1): 327-331. https://doi.org/10.1007/s00436-019-06527-z. PMid:31758297.

Salant H, Yasur-Landau D, Rojas A, Otranto D, Mazuz ML, Baneth G. *Troglostrongylus brevior* is the dominant lungworm infecting feral cats in Jerusalem. *Parasitol Res* 2020; 119(10): 3443-3450. https://doi.org/10.1007/s00436-020-06852-8. PMid:32813040.

Traversa D, Di Cesare A, Conboy G. Canine and feline cardiopulmonary parasitic nematodes in Europe: emerging and underestimated. *Parasit Vectors* 2010; 3(1): 62. https://doi.org/10.1186/1756-3305-3-62. PMid:20653938.

Traversa D, Morelli S, Di Cesare A, Diakou A. Felid Cardiopulmonary Nematodes: Dilemmas Solved and New Questions Posed. *Pathogens* 2021; 10(1): 30. https://doi.org/10.3390/pathogens10010030. PMid:33401704.

Traversa D, Morelli S, Di Cesare A, Strube C, Raue K, Bisterfeld K, et al. Efficacy of two topical combinations containing emodepside plus praziquantel, and emodepside plus praziquantel plus tigolaner, for the treatment of troglostrongylosis in experimentally infected cats. *Curr Res Parasitol Vector Borne Dis* 2022a; 2: 100097. https://doi.org/10.1016/j.crpvbd.2022.100097. PMid:35991087.

Traversa D, Raue K, Ringeisen H, Blazejak K, Bisterfeld K, Di Cesare A, et al. Efficacy of a spot-on combination containing 10% w/v imidacloprid and 1% w/v moxidectin for the treatment of troglostrongylosis in experimentally infected cats. *Parasit Vectors* 2022b; 15(1): 66. https://doi.org/10.1186/s13071-022-05185-y. PMid:35193656.

Umur Ş, Barılı Ö, Gencay Topçu EB, Gürler AT. First report of a *Troglostrongylus brevior* case in a domestic cat in Turkey. *Turkiye Parazitol Derg* 2020; 44(3): 176-178. https://doi.org/10.4274/tpd.galenos.2020.6889. PMid:32928727.

Supplementary Material

Supplementary material accompanies this paper.

Supplementary Figure S1. Left caudal (A), left perihilar (B), left middle (C), and left cranial (D) lung points, together with right caudal (E), right perihilar (F), right middle (G), and right cranial (H) lung points, recorded on day 84 following initiation of antiparasitic therapy. B lines (white arrowheads) and shred signs (white arrows) are noted.

Supplementary Figure S2. Left caudal (A), left perihilar (B), left middle (C), and left cranial (D) lung points, together with right caudal (E), right perihilar (F), right middle (G), and right cranial (H) lung points, recorded on day 140 following initiation of antiparasitic therapy. White arrows note the “A lines”.

This material is available as part of the online article from https://doi.org/10.1590/S1984-29612026050.